PAPER • **OPEN ACCESS**

Two-body dynamic simulations of a combined semi-submersible floating offshore wind turbine and torus wave energy converter

To cite this article: C F Lee *et al* 2023 *IOP Conf. Ser.: Mater. Sci. Eng.* **1294** 012007

Two-body dynamic simulations of a combined semi-submersible floating offshore wind turbine and torus wave energy converter

C F Lee*, V De Santis Tavares, M C Ong

Faculty of Science and Technology, University of Stavanger, Norway

* Correspondence: chern.f.lee@uis.no

Abstract. Dynamic responses of a combined wind and wave energy system which consist of a 5MW semi-submersible floating offshore wind turbine (FOWT) and a torus-shaped wave energy converter (WEC) are investigated. In the investigated configuration, the torus WEC is constrained to move only in the heave direction with respect to the FOWT. This results in a two-body dynamic system that allows for the extraction of wave energy through the relative heave motion. A Modelica-based multi-body system (MBS) code is used to perform fully coupled dynamic analyses of the combined system. The wind turbine loads are calculated using the state-of-the-art Blade Element Momentum (BEM) method, while the wave power take-off (PTO) system is modelled as a linear spring and a viscous damper. A case study is presented where the mass of the torus is varied to investigate the impact on the two-body dynamics of the combined system. The system performance is assessed in terms of the maximum wave power absorption and the quality of wind power production.

1. Introduction

The concept of harnessing wave energy as a viable energy source has been actively pursued since its inception more than 200 years ago. Over the years, many types of wave energy converter (WEC) designs, each varying in working principle and power-take off (PTO) mechanism have been proposed. Nonetheless, progress in wave energy technology has been sluggish, with limited consensus on an optimal shape or operating principle having been reached. Of the thousands of proposed concepts, only a few designs have reached the stage of commercialized deployment, far lower in number as compared to other renewable sources, such as solar energy and wind energy [1]. The current poor state of commercial utilization of wave energy technology can be attributed mainly to the difficulty in achieving high energy conversion efficiency over a range of wave amplitudes, phases, and directions [2]. Additionally, the extreme environmental loadings on the WEC structures can be 100 times higher than the average loadings, which can lead to overdesign of load bearing structures and subsequently a significant increase in the cost of energy [3].

To improve the chance of commercialization, one of the solutions that researchers have been investigating is to integrate WECs with floating offshore wind turbine (FOWTs) in the form of combined energy systems. The advantages of using such combined systems lie in the synergies between two different disciplines of energy production. To begin with, as wind and waves are statistically correlated, sites with high wind energy resources usually come with significant wave energy density which makes the combined concept a sensible solution. In addition, the integration of multiple energy devices onto a

single platform allows for higher energy production while sharing the same infrastructure, e.g., supporting structures, power cables, mooring systems, and substations. For a combined energy system, the motions of the floating platform can also be utilized to improve the performance of the WEC. Falnes [4] investigated the mechanism of wave energy conversion of a two-body WEC in heave mode and discovered that it is possible to achieve wave excitation forces on a two-body WEC that exceed those experienced by a single-body WEC. The conversion efficiency of a two-body WEC was also studied by Bijun Wu et al. [5]. It was found that the two-body motion characteristics are dependent on many parameters such as physical properties of the buoy and the incoming wave frequency. Liang and Zuo [6] described the dynamics of a two-body WEC by deriving the close-form solution of the power absorption as a function of mass and PTO parameters such as damping and stiffness. A notable commercial example of a two-body WEC is the Wavebob, developed by Wavebob Ltd. [7]. It uses the relative heave motion between the floating buoy and a second submerged body to extract wave energy. However, in 2013, the company was placed in liquidation being unable to attract sufficient financial investment [8].

To date, offshore wind technologies have reached a high technology readiness level, and a substantial reduction of 20% in the levelised cost of energy (LCOE) of offshore wind projects has been observed between 2010 and 2018 [9]. Taking advantage of the technological maturity of the wind industry, the combined exploitation of wave and offshore wind energy can potentially lead to a lower threshold of commercialization. This allows the wave energy technology development to accelerate with increased funding. The MARINA Platform project [10], which was funded by European Union (EU) shortlisted three floating wind and wave energy concepts for detailed investigation. The Spar-Torus-Combination (STC) [11], the Semi-submersible-Flap Combination (SFC) [12] and the combination of WindFloat semi-submersible wind turbine with an oscillating water column WEC array [13] make up the three characteristically different combined energy concepts. One of the common findings from the three concepts is that the introduction of WECs to a FOWT can modify the response characteristics of the floating platform. For the STC concept, Muliawan et al. [14] discovered that surge and pitch responses of the spar FOWT is reduced with the addition of a torus (donut-shaped) WEC, contributing to a stable pitch motion. Lee et al. [15] proposed a combined energy concept named STFC that integrates a semi-submersible FOWT with three flap type and one torus WECs. Their analysis showed that the presence of the WECs contributed to a reduced platform pitch motion and hence a reduction in wind turbine power fluctuation.

On the path towards complete commercialization of combined wind and wave energy systems, continued research is needed to improve conversion efficiency and to minimize the development costs. In this study, the two-body dynamics of a combined wind and wave energy system are investigated. A combined concept that integrates a column stabilized semi-submersible FOWT and a torus type WEC and is chosen as the case study, primarily due to its ease of integration and the straightforwardness of the wave power generation mechanism. To investigate the effect of torus buoy's physical properties on power absorption, the buoys with three different ballast mass are modelled. The performance of the combined system is compared in terms of wave power absorption and the resulting motion characteristic of the platform.

2. The combined wind and wave energy concept

The combined wind and wave energy concept in this study consists of a semi-submersible FOWT and a torus WEC as shown in Figure 1.

2.1. FOWT

The FOWT is of the 5-MW-CSC type that was originally proposed by Luan et al. [16] for a design water depth of 200 m. The braceless semi-submersible platform provides the motion stability and support required for the safe operation of a NREL 5-MW reference offshore wind turbine [17]. The supporting platform consists of four cylindrical columns of identical diameter, interconnected in a "Y" configuration via pontoons. The ballast water is distributed evenly across the pontoons and columns to

attain an operating draft of 30 m. Station-keeping of the CSC under environmental loadings is achieved through a 3-legged wire-rope-catenary mooring system. The specifications of the 5-MW-CSC platform is shown in Table 1.

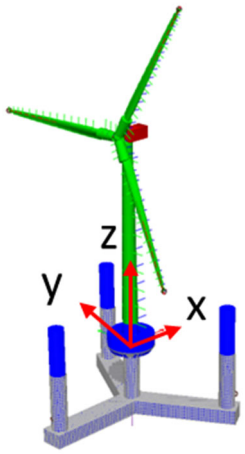

Figure 1. FOTW and Torus modelled in SIMA

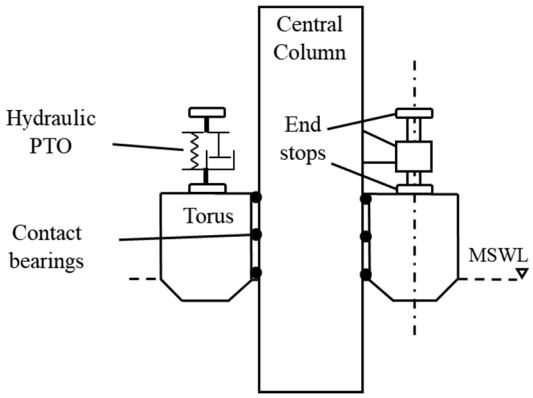

Figure 2. PTO mechanism of the torus WEC

Table 1. 5-MW-CSC platform specifications [16]

Draft (m)	30.0
Mass (kg)	9738000
Center of gravity (m)	-24.36
Center of buoyancy (m)	-22.48
Roll mass moment of inertia about COG (kg · m^2)	4.72E+09
Pitch mass moment of inertia about COG (kg · m^2)	4.72E+09
Yaw mass moment of inertia about COG (kg · m^2)	8.24E+09

2.2. Torus WEC

The torus WEC comprises of two components; (1) a torus buoy installed through the central column of the FOWT and (2) the PTO system and mechanical connections. The PTO and mechanical connections facilitate the constrained relative motion between the buoy and the CSC. In its neutral position, the torus buoy is freely floating with a 2 m draft. The physical dimensions and properties of the torus WEC have been estimated according to published information of the STC [14,18]. Through contact bearings fitted around the inner diameter of the torus, it is constrained to move together with the CSC in surge, sway, roll, pitch and yaw. The PTO system, consisting of hydraulic cylinders and the hydraulic circuit converts the torus's heave motion into usable power. Mechanical end stoppers are used to limit the torus's heave motion to ±3 m in relation to the FOWT. The PTO mechanism of a torus WEC is illustrated in Figure 2. The power absorbed by the torus WEC can be derived from the relative heave velocity, v_{rel} between the CSC and the torus given by,

$$P_{\mathrm{Torus}} = B_{\mathrm{PTO}} \cdot v_{\mathrm{rel}}^2(t) \quad (1)$$

where B_{PTO} is the PTO damping coefficient. The PTO system in the present study utilizes a passive (constant damping and stiffness) control strategy which sees the force exerted by the PTO being represented by

$$F_{\text{Torus}}(t) = -B_{\text{PTO}} \cdot v_{\text{rel}}(t) - K_{\text{PTO}} \cdot x_{\text{rel}}(t) \quad (2)$$

where K_{PTO} is the PTO spring stiffness and x_{rel} is the relative heave position between the CSC and the torus. One of the primary limitations of passive control strategies is that they are pre-tuned to optimize energy absorption within a narrow frequency range. However, while passive control strategies are no longer considered state-of-the-art in modern WEC controllers, they remain a choice for developers willing to test a WEC at an industrial scale due to their ease of implementation and operational safety. Given the focus of this study on examining the impact of varying torus mass on WEC performance, a passive damping control strategy is employed.

Three tori with different ballast masses are modelled to investigate its effect on platform motions and power absorption. The difference in mass is achieved through ballasting of the tori to different draft levels. Slight modifications to the tori's submerged geometries as shown in Figure 3 are made in order to limit the change in hydrodynamic coefficients (added mass and potential damping) to a minimum. Table 2 provides a summary to the properties of the tori investigated in this study.

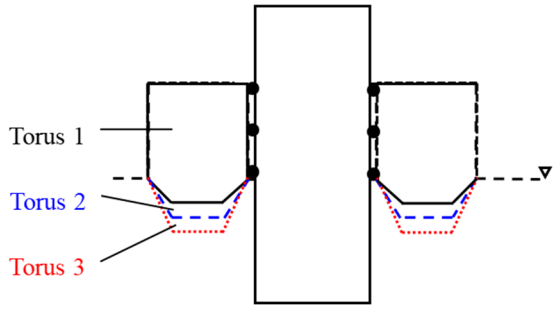

Figure 3. Comparison of submerged geometries for the three tori

Table 2. Torus specifications

	Torus #1	Torus #2	Torus #3
Draft (m)	2.0	2.5	3.0
Torus mass (kg)	423766	529710	635654
Center of gravity (m)	0.92	0.11	-0.52
Center of buoyancy (m)	-0.91	-1.13	-1.36
Roll mass moment of inertia about COG ($\text{kg} \cdot \text{m}^2$)	1.71E+07	2.04E+07	2.36E+07
Pitch mass moment of inertia about COG ($\text{kg} \cdot \text{m}^2$)	1.71E+07	2.04E+07	2.36E+07
Yaw mass moment of inertia about COG ($\text{kg} \cdot \text{m}^2$)	2.62E+07	3.21E+07	3.82E+07

3. Dynamic modelling and analysis of the combined concept

The combined concept is modelled using OpenModelica (OM), an open-source platform based on the Modelica language developed by the Open Source Modelica Consortium [19]. Using OM as the primary platform for development, the fully coupled aero-hydro-servo-elastic framework for the dynamic analysis of FOWT is described by El Beshbichi et al. [20].

3.1. Aerodynamics

The Blade Element Momentum (BEM) method as described by Glauert [21] is the most commonly used tool for calculating aerodynamic loads on wind turbine rotors due to it being computationally inexpensive while preserving reasonable accuracy. In the present study, the BEM calculations are implemented through AeroDyn v15, the wind turbine aerodynamic module within NREL's FAST v8.2

[22]. AeroDyn calculates wake influence on the wind turbine based on quasi-static BEM theory which means that the induction factors react instantaneously to the change in aerodynamic loads. In the BEM solution, the Glauert's empirical correction is applied for high axial induction factors while Prandtl tip-loss, Prandtl hub-loss, and Pitt and Peters skewed-wake are applied to account for the corrections due to 3-dimensional (3D) effects. Turbulent wind inputs are generated using TurbSim [23], a stochastic inflow turbulence tool by NREL.

3.2. Hydrodynamics

The hydrodynamic loads on the submerged body are calculated based on the linear wave theory. Frequency-domain hydrodynamic analysis is carried out using DNV's Wadam software [24] to compute the added mass, potential damping coefficients and first-order wave force transfer functions. In the present study, the added mass and potential damping couplings between CSC and the torus are assumed to be negligible. The calculations of first-order wave force transfer functions for the CSC take into account the presence of the torus, and similarly, the calculations of first-order wave force transfer functions for the torus consider the presence of CSC.

3.3. Mooring line dynamics

The station-keeping capability is achieved through the implementation of a quasi-static mooring line module for each mooring line. With the fairlead positions known at each time instance, the mooring line module solves for and output the tensions at fairleads, assuming that the mooring lines are in static equilibrium during each simulation time step.

3.4. Connections between the FOWT and torus

In OM, the contact between CSC and the torus is modelled as a cylindrical joint which allows for relative motion in the heave direction. In SIMA, however, the contact is realized using the "docking cone and pin" feature [25]. This feature keeps the torus and the center column of the CSC axially aligned by applying a restoring force that is a function of the radial offset. The PTO is modelled as a linear damper with damping coefficient of 8000 kNs/m and a linear spring with stiffness of 10 kN/m in parallel. The tuning of the PTO is according to the values suggested by Muliawan et al. [14].

3.5. Rigid body and structural dynamics

A multi-body approach is employed to model the floater dynamics and the wind turbine structural dynamics of the combined system. The floaters (CSC and torus) are modelled as rigid bodies with concentrated masses. The equations of motion of the rigid floaters can be given by,

$$[M + A_\infty]\ddot{q} + \int_0^t [K(t-\tau)]\,\dot{q}\,d\tau + [C]q = [F]_{\text{waves}} \tag{3}$$

where $[M]$ is the mass matrix, $[A_\infty]$ is the infinite frequency added mass matrix, $[K]$ is the wave-radiation-retardation kernel matrix, $[C]$ is the restoring coefficient matrix, $[F]_{\text{waves}}$ is the first-order wave force and q, $\dot{q}$, $\ddot{q}$ are the position, velocity and acceleration of the floaters, respectively. The wind turbine tower and blades are discretized as generalized beam elements (GBE) assuming small, linear, and elastic structural deformations. For each GBE, longitudinal, transverse, and torsional degrees-of-freedom (DOFs) are considered each with the corresponding stiffness values. More information on the modelling of structural dynamics can be referred to the work by El Beshbichi et al. [20].

4. Results and discussion

The numerical model established in OM is first validated against an identical twin created in SIMA, a dynamic analysis software developed by SINTEF Ocean [25,26]. Based on the validated model, the combined systems with different torus masses are simulated in regular wave conditions. One representative irregular waves and turbulent wind environmental condition (EC) is also simulated to look at the average hourly-power production of the WEC.

4.1. Code-to-code validation study

In the present study, regular waves with thirteen different wave periods as shown in Table 3 are simulated. Figures 4, 5, 6 and 7 show the resulting surge, heave, pitch and absorbed power response amplitude operators (RAOs), respectively, for the numerical models developed in OM and SIMA. Only the case with Torus no.1 is used in the validation study.

Table 3. Wave periods used for validation study and regular wave simulations in OM and SIMA

Wave periods (s)												
5.01	6.97	7.93	8.91	9.89	10.86	11.83	12.81	13.78	14.76	15.73	17.68	19.74

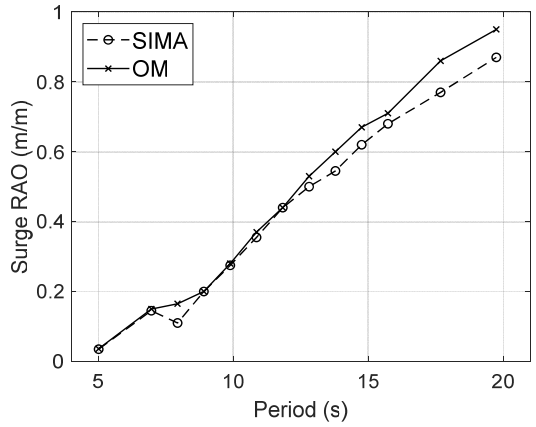

Figure 4. Surge RAO of the platform in SIMA and OM.

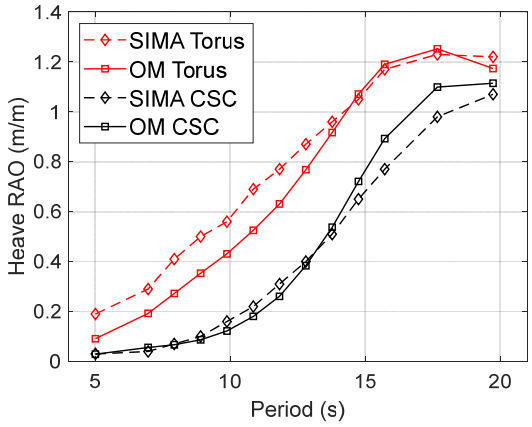

Figure 5. Heave RAO of the platform and torus in SIMA and OM.

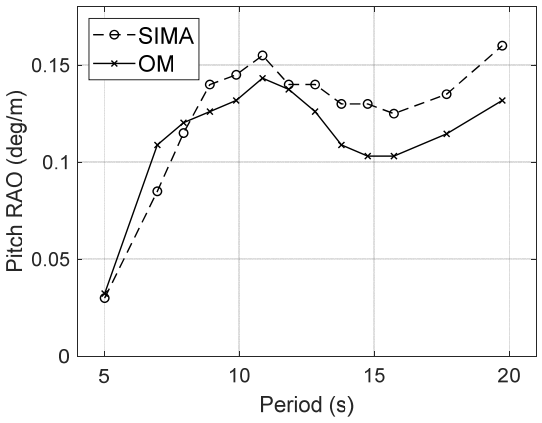

Figure 6. Pitch RAO of the platform in SIMA and OM.

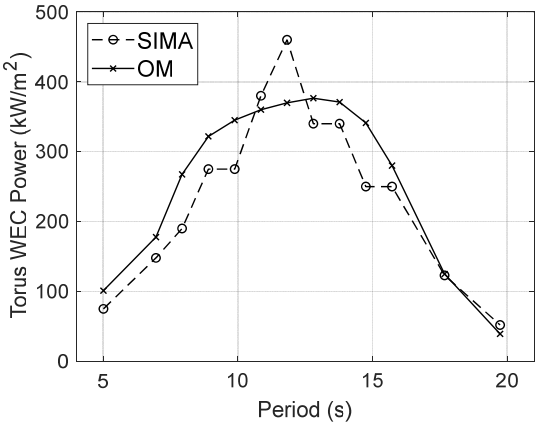

Figure 7. Absorbed power RAO of the WEC in SIMA and OM.

As shown in Figures 4 and 5, the surge and heave RAO values calculated by OM and SIMA are in close agreement. As compared to surge and heave RAOs, larger discrepancies are observed between the pitch RAO values estimated using different tools (Figure 6), and this is due to the difference in which the contact between the platform and torus is modelled. For the model in SIMA, the torus is allowed to have a slight relative pitch motion with respect to CSC while in OM, the torus follows CSC in pitch. In any case, within the investigated wave frequency range, pitch RAOs are in general less than 0.2° and

thus the discrepancies are deemed insignificant for the purpose of this study, which revolves primarily around the heave DOF. As shown in Figure 7, the absorbed power RAO of the torus WEC peaks when the system is excited by regular waves with a period of approximately 12 s. Within the resonance frequency range, the absorbed power RAO calculated using SIMA are of higher values as compared to those calculated using OM. This can be attributed to a much-restricted pitch motion for the torus modelled in OM as shown in Figure 6.

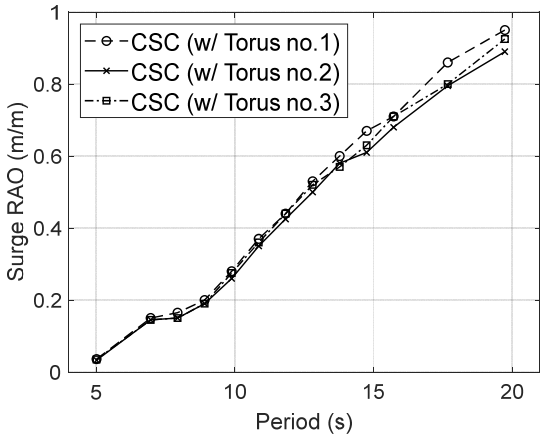

Figure 8. Surge RAO of the platform with three different torus masses

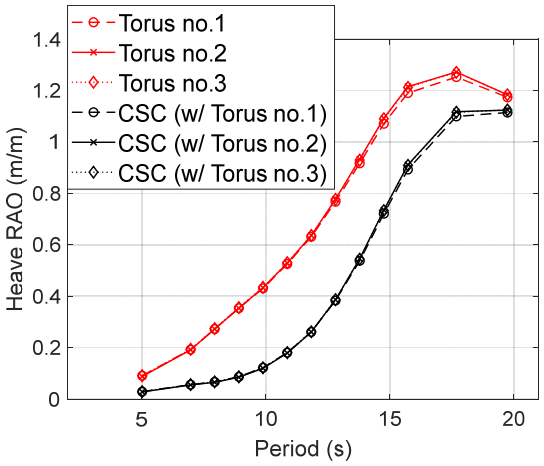

Figure 9. Heave RAO of the platform and the tori with three different masses

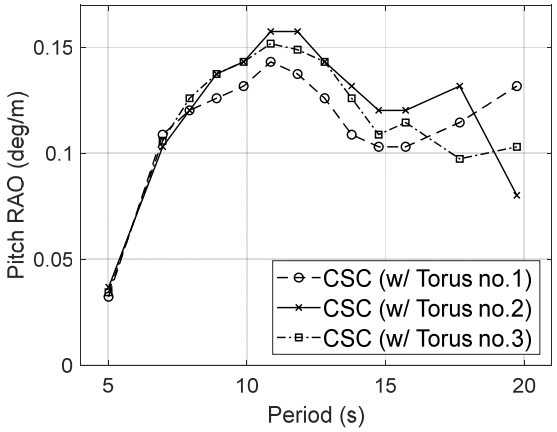

Figure 10. Pitch RAO the platform with three different torus masses

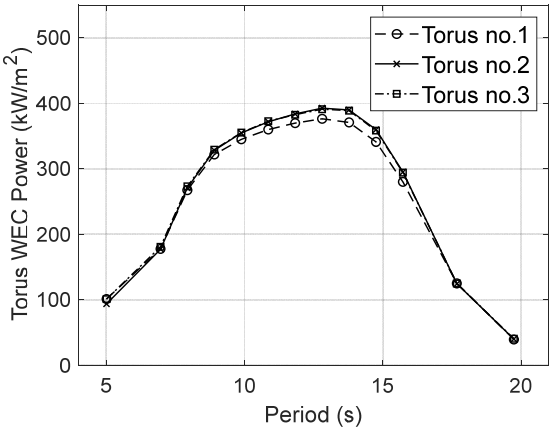

Figure 11. Absorbed power RAO of the WEC with three different torus masses

4.2. Regular wave simulations

In this section, regular wave simulations with the same wave periods as listed in Table 3 are carried out for the combined system by varying the torus properties (Torus no.1 is replaced with Torus no.2 and Torus no.3). The RAOs for the platform surge, platform heave, torus heave and platform pitch motions and the power absorbed by the PTO for the three investigated cases are compared in Figures 8 – 11, respectively.

As shown in Figures 8 and 9, the motions in the surge and heave DOFs are not significantly affected by the change in torus mass as the motion characteristics in these DOFs are influenced by the mooring system and the platform geometry of CSC. In pitch, the platform oscillates with higher RAO values with Torus 2 and Torus 3 as compared to Torus 1 as shown in Figure 10, with the pitch RAO of the platform

with Torus 2 being the highest. This directly affects the absorbed power RAOs. As shown in Figure 11, with a wave period of approximately 13 s, a 6% increment in the absorbed power RAO is observed for the combined energy system with Torus no. 2.

4.3. Irregular waves and turbulent wind simulations

In this section, the combined energy system with three different torus masses is simulated in an irregular wave and turbulent wind condition. The selected sea state is based on the wind-wave joint probabilistic model proposed by Johannessen et al. [27] and has a significant wave height, H_s of 2.10 m and a peak period, T_p of 9.74 s. Three-dimensional turbulent wind fields of 5 m/s wind speed at wind turbine hub height are generated according to IEC Class C of the Kaimal turbulence model. Wind and waves are directionally aligned pointing in the positive x-direction as shown in Figure 1. Finally, to account for statistical variation, six random wind and wave realizations are simulated for the EC.

Figures 12, 13 and 14 show the average statistics of platform surge, platform heave, torus heave and platform pitch motions each presented in terms of mean offset and standard deviation of the corresponding motion. The platform's motion in surge is governed mainly by the mooring system. Hence, the mean offset and standard deviation for the platform surge motion remain largely unchanged when the torus mass increases as shown in Figure 12. Similar to the surge motion, the change in torus mass does not result in significant change in platform pitch motion as shown in Figure 13. This is due mainly to the unchanged water plane area (the water plane areas for all tori are the same). Figure 14 shows that the mean and standard deviation of the tori's heave motions are significantly higher than the platform. With a higher torus mass, an increase in torus heave standard deviation is observed. However, as the torus mass is increased further (from torus no.2 to torus no.3), smaller heave responses are detected for both CSC and the torus. This indicates that, with the current PTO parameter tuning, the mass ratio between CSC and torus no.2 reaches an optimal level.

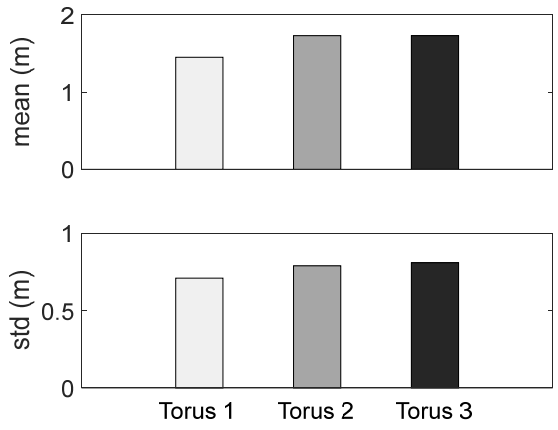

Figure 12. Platform surge motion statistics with three different torus masses

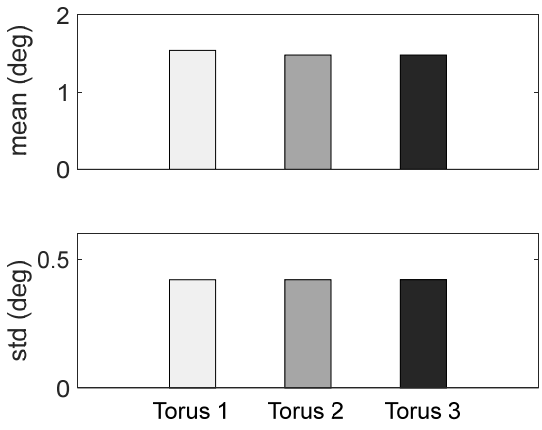

Figure 13. Platform pitch motion statistics with three different torus masses

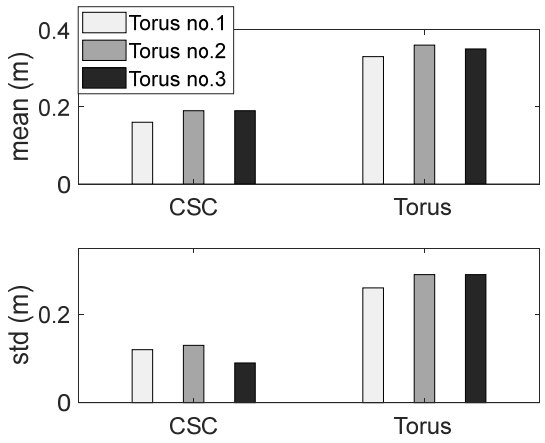

Figure 14. Platform and torus heave motion statistics with three different torus masses

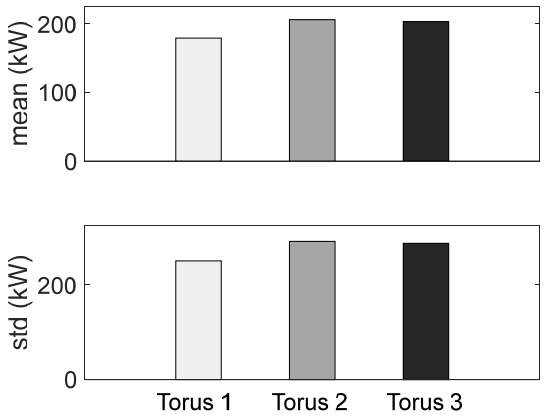

Figure 15. Absorbed power statistics for the WEC with three different torus masses

Figure 15 shows the average statistics of the WEC absorbed power. An increase in torus motion standard deviations as shown in Figure 14 directly results in an increase in mean absorbed power. For the investigated EC, the mean absorbed power of the combined system with Torus no. 2 and Torus no.3 increase by 15% and 14%, respectively. This increase in mean absorbed power is accompanied by an increase in the absorbed power standard deviation of approximately 15%. It can therefore be concluded that a smaller mass difference between the torus and platform will improve the performance of the combined wind and wave energy system in terms of wave power extraction.

5. Conclusion

A combined wind and wave energy system, consisting of a semi-submersible and a torus WEC, is proposed in the present study. The numerical model developed in OM is first validated using SIMA by comparing the results in regular wave simulations. Satisfactory agreement is found between the results calculated by OM and SIMA. To explore the impact of increasing torus mass on the platform's motion characteristics and the WEC's power absorption, two additional torus designs with different ballast masses have been introduced. RAO results show an increase in power absorption as the torus mass is increased while the platform motions remain insensitive to the increase in torus mass. One sea state is used to investigate the performance of the combined system in irregular waves and turbulent wind environmental conditions. With passive control system, it can be observed that an increase in torus mass positively impacts WEC power absorption, with a 15% rise in 1-hour mean power absorption under the examined environmental condition. Further improvements to the WEC system such as the implementation of a more advanced control system, further tuning of the control parameters (for each torus mass) and the optimization of torus shape are among the subjects for future studies.

References

[1] Aderinto T and Li H 2018, Ocean wave energy converters: status and challenges, *Energies*, **11**(5), 1250.
[2] Czech B and Bauer P 2012, Wave energy converter concepts: design challenges and classification", *IEEE Industrial Electronics Magazine*, 6(2), 4-16.
[3] Cruz J 2008, *Ocean Wave Energy: Current Satus and Future Perspectives*, Springer Berlin, Heidelberg.
[4] Falnes J 1999 Wave-energy conversion through relative motion between two single-mode oscillating bodies, *J. Offshore Mech. Arctic Eng.* **121**, 32-38.
[5] Wu B, Wang X, Diao X, Peng W and Zhang Y 2014, Response and conversion efficiency of two

degrees of freedom wave energy device, *Ocean Eng.* **76**, 10-20.
[6] Liang C, Zuo L, 2017 On the dynamics and design of a two-body wave energy converter. *Renewable Energy*, **101**, 265-274.
[7] Weber J, Mouwen F, Parish A and Robertson D 2009, Wavebob – research and development network and tools in the context of systems engineering, Proc. 8th European Wave and Tidal Energy Conference, Uppsala, Sweden.
[8] O'Halloran B, 2013, Ocean energy developer wavebob set to go under, The Irish Times, Ireland.
[9] Jiang Z, 2021 Installation of offshore wind turbines: A technical review, *Renewable and Sustainable Energy Rev.* **139**, 110576.
[10] Sojo M and Auer G 2014 Deliverable D1.12 Final Summary Report, Marine Renewable Integrated Application (MARINA) Platform.
[11] Muliawan M J, Karimirad M, Moan T, and Gao Z 2012 STC (Spar-Torus Combination): a combined spar-type floating wind turbine and large point absorber floating wave energy converter – promising and challenging", *Proc. of the ASME 31st Int. Conf. on Ocean, Offshore and Arctic Eng*., Rio de Janeiro, Brazil.
[12] Luan C, Michailides C, Gao Z, and Moan T 2014 Modeling and analysis of a 5 MW semi-submersible wind turbine combined with three flap type wave energy converters, *Proc. of the ASME 33rd Int. Conf. on Ocean, Offshore and Arctic Eng.*, San Francisco, California, USA.
[13] O'Sullivan K P 2014 Feasibility of Combined Wind-wave Energy Platforms, Ph.D. thesis, National University of Ireland, Ireland.
[14] Muliawan M J, Karimirad M and Moan T 2013 Dynamic response and power performance of a combined Spar-type floating wind turbine and coaxial floating wave energy converter, *Renewable Energy*, **50**, 47-57.
[15] Lee C F, Tryfonidis C and Ong, M C 2022 Power performance and response analysis of a semi-submersible wind turbine combined with flap-type and torus wave energy converters, *J. Offshore Mech. Arctic Eng.*, **145**(4), 042001.
[16] Luan C, Gao Z, and Moan T 2016 Design and analysis of a braceless steel 5-mw semi-submersible wind turbine, *Proc. of the ASME 35th Int. Conf. Ocean, Offshore Arctic Eng*., Busan, South Korea.
[17] Jonkman J, Butterfield S, Musial W and Scott G 2009 Definition of a 5-MW Reference Wind Turbine for Offshore System Development, NREL/TP-500-38060, NREL, CO, USA.
[18] Wan L, Gao Z and Moan T 2014 Dynamic response and power performance of a combined Spar-type floating wind turbine and coaxial floating wave energy converter, *Proc. ASME 33rd Int. Conf. Ocean, Offshore Arctic Eng.*, San Francisco, California, USA, 9A, V09AT09A010. DOI: 10.1115/OMAE2014-23213
[19] OSMC, 2021, OpenModelica User's Guide. Release v1.19.0.
[20] El Beshbichi O, Xing Y and M C Ong 2023, Modelica-AeroDyn: Development, benchmark, and application of a comprehensive object-oriented tool for dynamic analysis of non-conventional horizontal-axis floating wind turbines, *Wind Energy*, **26**(6), 538-572.
[21] Glauert H, 1963 Airplane propellers, W.F. Durand (Ed.), Aerodynamic theory, Dover Publications, New York.
[22] Moriarty P J and Hansen A C 2005 AeroDyn Theory Manual, NREL/TP-500-36881, NREL, CO, USA.
[23] Jonkman B J 2009 TurbSim User's Guide: Version 1.50, NREL/TP-500-46198, NREL, CO, USA.
[24] DNV, 2013, SESAM User Manual HydroD, Det Norske Veritas, Oslo, Norway.
[25] SINTEF Ocean, 2017, SIMO 4.10.1 User Guide, SINTEF Ocean: Trondheim, Norway.
[26] SINTEF Ocean, 2017, RIFLEX 4.10.1 User Guide, SINTEF Ocean: Trondheim, Norway.
[27] Johannessen K, Meling T S and Haver S 2002, Joint distribution for wind and waves in the northern North Sea, *Int. J. Offshore Polar Eng*., **12**(2).